HHS Public Access

Author manuscript

Magn Reson Med. Author manuscript; available in PMC 2018 June 01.

Published in final edited form as:

Magn Reson Med. 2017 June ; 77(6): 2296–2302. doi:10.1002/mrm.26325.

Fast Measurement of Blood T_1 in the Human Carotid Artery at 3 Tesla: Accuracy, Precision and Reproducibility

Wenbo Li[1,2], **Peiying Liu**[1], **Hanzhang Lu**[1], **John J. Strouse**[3], **Peter C.M. van Zijl**[1,2], and **Qin Qin**[1,2]

[1]Department of Radiology; Johns Hopkins University School of Medicine, Baltimore, Maryland, USA

[2]F.M. Kirby Research Center for Functional Brain Imaging, Kennedy Krieger Institute, Baltimore, Maryland, USA

[3]Division of Pediatric Hematology, Department of Pediatrics, Johns Hopkins University School of Medicine, Baltimore, Maryland, USA

Abstract

Purpose—To develop a fast protocol for measuring T_1 values in the internal carotid artery (ICA), to validate this technique with *in vitro* measurements, and to evaluate its reproducibility.

Methods—A modified Look-Locker sequence was optimized to enable rapid determination of T_1 in the ICA at 3T. T_1 values from the ICA were compared with *in vitro* measurements on individually sampled venous blood oxygenated to arterial levels. A test-retest reproducibility study was also conducted.

Results—The group-averaged arterial blood T_1 value was 1908+/−77 ms for 6 female adults (hematocrit = 0.39+/−0.03) and 1785+/−55 ms for 7 male adults (hematocrit = 0.45+/−0.02), which is 100–200 ms longer than the widely adopted value obtained from bovine blood experiments. The arterial T_1 value per subject correlated significantly with individual hematocrit (Hct) values. The intra-session and inter-session coefficients of variation (CoV) were 1.1% and 2.1% respectively, indicating good precision and reproducibility of our method. Reasonable agreement was observed between the *in vivo* and *in vitro* results with a correlation coefficient of 0.78.

Conclusion—The proposed method can provide fast arterial T_1 measurement on individual subjects. When not performing such a subject-specific measurement, we recommend the use of 1908 ms and 1785 ms for healthy female and male adults, respectively, or 1841 ms for adults in general.

Corresponding author: Qin Qin, PhD, Department of Radiology, Johns Hopkins University School of Medicine, F.M. Kirby Research Center for Functional Brain Imaging, Kennedy Krieger Institute, 707 N. Broadway, Baltimore, MD, 21205, qin@mri.jhu.edu, Tel: 443-923-9516, Fax: 443-923-9505.

Introduction

The T_1 value of arterial blood is an important parameter for the quantification of cerebral blood flow (CBF) using arterial spin labeling (ASL) techniques (1). It is also critical in VASO experiments for relative cerebral blood volume (CBV) (2,3) or absolute arterial CBV (4,5) determination. Standard practice is to assume a constant arterial blood T_1 across all individuals (6). However, blood T_1 is known to have dependence on hematocrit (Hct) (7–19) (e.g. due to individual variation or in anemia or polycythemia), oxygenation fraction (Y) (9,11,13,16–25) (e.g. in hypoxemia or ischemia), the age of subject (7,8,16), and blood composition (26) (e.g. in sickle cell disease). Therefore, a fast protocol to measure individual arterial blood T_1 in vivo is desirable to accurately calculate CBF.

A modified Look-Locker scheme (7,8,12,15,27–29) has been proposed with a non-selective inversion pulse followed by a train of slice-selective readouts, through which multiple inversion time points can be acquired rapidly due to constant refreshing of blood. This method has been applied to measure Gd-dosed blood T_1 in renal arteries and veins (27,28) and venous blood T_1 in the sagittal sinus (8,15,29) and internal jugular vein (IJV) (12). However, the application of this approach to measure arterial blood T_1 suffers from the poor inversion efficiency for the arterial blood magnetization in the chest area, which is due to large B_0 and B_1 inhomogeneities and flow artifacts associated with the faster and more pulsatile flow of arterial blood.

In this work, we optimized our previous IJV-based T_1 protocol (12) to measure blood T_1 in the internal carotid artery (ICA), verified the accuracy of the results with in vitro experiments on individually sampled blood, and evaluated the precision and reproducibility of the new method with a test-retest study.

Methods

Fast T_1 Measurement in the ICA

The pulse sequence for measuring arterial blood T_1 at ICA was similar to the sequence used previously to measure venous blood T_1 at IJV (12), namely a nonselective adiabatic inversion pulse followed by multiple imaging acquisition blocks separated by short time intervals (T_d) (Fig. 1a). The main difference between a T_1 measurement at the ICA and IJV is the positioning of subjects relative to the RF body coil. The regular neuroimaging setup (centering at eye level) is sufficient for an IJV T_1 measurement, because the normal cerebral mean transit time (from ICA to IJV) is close to the TR ~ 10 s (30). Therefore all venous blood entering the IJV is within the brain when the inversion pulse is applied (12). For subjects without heart disease, the mean transit time from pulmonary artery to ICA is close to 8 sec (31,32). To acquire proper inversion recovery curves for the fast flowing arterial blood at the ICA, it is crucial to invert all of the incoming blood magnetization from the heart, lung, aorta, common carotid and ICA. Since the body coil length of the scanner used in this study was 65 cm, subjects needed to be positioned in the middle between ICA and diaphragm, i.e. the clavicle, to have all the feeding blood covered by the RF coil (Fig. 1b).

In addition, due to the larger B_0 and B_1 inhomogeneities in the chest area, the bandwidth of the standard hyperbolic secant (HS) adiabatic pulse (33) (10 ms, 1250 Hz bandwidth) used in the IJV T_1 protocol (12) did not achieve uniform inversion for the arterial T_1 measurement. HSn adiabatic pulses (34,35), which modify the HS pulse by raising the time variable in the sech function to a higher *n*th power leading to higher bandwidth, were investigated for better performance. Numerical simulations using the Bloch equations based on matrix rotation were conducted to assess the inversion efficiencies of different adiabatic pulses over a wide range of B_0/B_1 conditions: B_0 field: ±2000 Hz; B_1^+ scale (ratio of actual flip angle to nominal input flip angle): from 0.0 to 2.0. Based on the simulation results, a 20 ms HS4 inversion pulse ($n = 4$, $\beta = 4$) was employed for in vivo experiments for its superior performance with 2500 Hz bandwidth through a large B_1^+ scale range from 0.4 to 2.0 (Supporting Fig. S1).

In Vivo Experiments

Experiments were performed on a 3T Philips Achieva scanner (Philips Medical Systems, Best, The Netherlands) using the body coil for RF transmission (maximum B_1 amplitude 13.5 μT) and a 32-channel head coil for signal reception. Thirteen healthy volunteers (6 females, age: 35+/−9, 7 males, age: 35+/−6 years) participated in this study after providing informed written consent in accordance with the local Institutional Review Board guidelines.

As part of the scan planning, a survey image was acquired in the coronal plane to visualize the upper torso. A quick 3D Time-of-Flight (TOF) scan (0.5 min) was employed in the neck to visualize the location of neck vessels, including internal carotid arteries, external carotid arteries, and vertebral arteries. The field of view (FOV) was 180 × 160 × 99 mm^3, the acquisition matrix was 180 × 159, and the reconstruction resolution was 0.94 × 0.93 × 3 mm^3.

For the arterial blood T_1 measurements, an imaging plane of thickness (THK) = 5 mm was placed at the level of foramen magnum and perpendicular to one side of ICA above the bifurcation of the common carotid to reduce artifacts from the turbulence of arterial blood, as detailed in a previous study (36). The acquisition parameters were: FOV = 140 × 169 mm^2, acquisition matrix = 176 × 204, with left-right phase encoding. The in-plane resolution after reconstruction was 0.76 × 0.75 mm^2. Segmented turbo field echo (TFE) acquisition, instead of segmented EPI used previously (12), was chosen for its improved robustness against motion artifacts from arterial blood pulsation. The full k-space at each inversion time (TI) was acquired with 15 k-lines per segment (TFE factor = 15, low-high profile ordering), SENSE factor = 2, $N_{shot} = 7$. With flow compensation and TR/TE = 13/7.6 ms, the acquisition window (T_{acq}) was about 195 ms. The first TI was sampled at TI(1) = 160 ms and the others were acquired at intervals of 285 ms. Note that the gap between adjacent TFE acquisition blocks (T_d) should be longer than the time (THK/v) required for blood flowing through the slice with velocity v (Fig. 1a), in order to remove any spin history of previous excitations so that the inflowing spins are only affected by the inversion pulse (12). Using the previously measured velocity in the IJV (v = 16 cm/s) (12) as an estimate of the lower limit of the velocity at ICA, the threshold for the replenishing time for THK = 5 mm is 31

ms, which is much shorter than T_d = 90 ms. With a total of 34 TIs recorded, total TR per shot (TR_{shot}) was 9850 ms, leading to a total acquisition time of about 1 min.

Different excitation flip angles (10°, 30°, 50°, 70°, 90°) for the TFE acquisition were compared among 4 subjects. Higher flip angles suppressed the background static tissue better (Supporting Fig. S2a–e) as expected; the measured arterial T_1 values using these various flip angles were found consistent (Supporting Fig. S2f). Considering both signal-to-noise ratio (SNR) and specific absorption rate (SAR), 50° flip angle was chosen in the remaining experiments.

The reproducibility of this protocol was evaluated by scanning each volunteer in two sessions, one in the morning and another in the afternoon with a separation of 3–6 hours. During each session, T_1 measurements at ICA (subject centering at the clavicle) were each performed twice consecutively, using the acquisition protocol described above. Meanwhile, T_1 measurement at the IJV were also performed in every session based on previous protocol (12).

In Vitro Experiments

A subgroup of volunteers (6 females, 3 males, age: 35+/−8 years old) had their blood drawn right before or after their first MRI scans. Two 4mL tubes of venous blood were collected at the outpatient clinic of Johns Hopkins Hospital. One tube of blood (anticoagulated with K_2EDTA) was sent to the hospital's pathology lab for a complete blood count (CBC). A second tube of blood (anticoagulated with lithium heparin) was brought back to our MRI center for the in vitro experiments on the same day, in order to validate the in vivo measurements. Before the MRI scans, the blood sample was oxygenated to 96%–99% through exposing it to the air typically for ~20 mins. After determining the oxygenation fraction (Y) and methemoglobin fraction (f_{MetHb}) concentration using the blood analyzer (ABL800, Radiometer), the sample was sealed in a tube with a diameter of 1 cm and equilibrated to 37.8°C.

A conventional inversion-recovery sequence (Supporting Fig. S3a) with TI = [0.2, 0.5, 1, 2, 3, 5, 9, 15] s was employed for the in vitro measurement of blood T_1. To ensure a constant initial magnetization before the inversion pulse for different TIs, a non-selective tailored hard-pulse saturation pulse train (65°, 83°, 143°, 162°) (37) following the acquisition reset the remaining magnetization to zero and a fixed delay of 2 s was inserted. Two-shot TFE (flip angle = 8°, TR/TE = 15/2.5 ms, TFE factor = 20, Tacq = 110 s) was used to acquire the 2D image of THK = 3 mm with the FOV of 64 × 120 mm^2 and resolution of 0.94 × 0.94 mm^2. The scan time was kept to within 2 min to prevent erythrocyte sedimentation. During the scan, the blood tube was placed in a 37.8 °C water bath (Supporting Fig. S3b,c) (16). For signal reception, a 2-channel shoulder coil was used and stabilized by foam pads. After the experiment, the temperature of the blood was measured (36.3–36.6 °C) and the oxygenation and lack of precipitation of erythrocytes were confirmed.

Data Analysis

Matlab (MathWorks, Inc., Natick, MA, USA) was used for simulation and data processing. ROIs were manually drawn on the images acquired at the longest TI and applied to images at other TIs.

It is important to point out that the slow flow near the vessel wall could make the fitted T_1 shorter if the blood in the imaging plane can not be refreshed before the next TFE acquisition block. Besides shortening T_1, such slow flow and partial volume effects with non-flowing water spins in surrounding tissue also reduce the imaging intensity for this thin layer. Therefore, for in vivo data, the center of the ICA vessels with higher signal were chosen as ROIs to avoid partial volume effect from the static tissue and the layer of blood with much slower velocity near the vessel wall. The averaged magnitude intensity of each ROI was fitted as a function of TI using the nonlinear-least-square algorithm for a 3-parameter model (12): the initial magnitude S_0, the inversion degree α and the blood T_1.

$$S(TI)=S_0|1-2\alpha e^{-TI/T_1}+e^{-TR_{shot}/T_1}| \quad [1]$$

For in vitro data with long TR, blood T_1 was fitted using a 2-parameter model (9), where C is related to saturation delay time and inversion efficiency:

$$S(TI)=S_0|1-Ce^{-TI/T_1}| \quad [2]$$

In order to evaluate the reproducibility of our method, the coefficient of variation (CoV) for intra-session, inter-session and inter-subject were calculated as:

$$CoV_{IntraSession}=\frac{1}{I\times J}\sum_{i=1}^{I}\sum_{j=1}^{J}\frac{|T_1^{ij1}-T_1^{ij2}|}{\sqrt{2}\cdot Mean(T_1^{ij1},T_1^{ij2})} \quad [3]$$

$$CoV_{InterSession}=\frac{1}{I\times K}\sum_{i=1}^{I}\sum_{k=1}^{K}\frac{|T_1^{i1k}-T_1^{i2k}|}{\sqrt{2}\cdot Mean(T_1^{i1k},T_1^{i2k})} \quad [4]$$

$$CoV_{InterSubject}=\frac{1}{J\times K}\sum_{j=1}^{J}\sum_{k=1}^{K}\frac{STD_i(T_1^{ijk})}{Mean(T_1^{1jk},T_1^{2jk})} \quad [5]$$

where T_1^{ijk} represents the *k*th measurement of blood T_1 value at participant *#i* in session *#j*. I, J, and K were total number of participants, sessions and measurement times in one session, respectively. $STD_i(T_1^{ijk})$ stands for the standard deviation of T_1 values for all the subjects at the *k*th measurement in session *#j*.

Results

Fig. 1b–d show typical localization of the imaging slice for the T_1 measurement at ICA, prescribed on both the anatomical (Fig. 1b) and angiographic images (Fig. 1c). When subjects were centered at the clavicle, reasonable inversion recovery data (Supporting Fig. S4) and arterial blood T_1 values were obtained for the ICA (Fig. 2a, red curve). However, when subjects were centered at the eye level, the inflow of non-inverted fresh blood reduced the measured T_1 at ICA notably (Fig. 2a, black solid curve). Fig. 2b compares results using a 10 ms HS pulse with bandwidth = 1250 Hz (black dash curve) and a 20 ms HS4 pulse with bandwidth = 2500 Hz (red solid curve). The HS4 pulse with much larger B_0/B_1 tolerance (Supporting Fig. S1) yielded more acceptable T_1 values from ICA blood (Fig. 2b). It is worth noting that any metal in necklaces and the bra (breast retainment apparatus), which did not cause problems for T_1 measurements at IJV, were found to hugely affect the B_0 inhomogeneity in the chest area and thus demand removal before scans. No motion artifacts were observed for any data sets.

Table 1 reports the hematocrits (Hct) and hemoglobin concentrations in whole blood (ctHb) from the CBC tests, along with the arterial and venous T_1 values of each subject averaged from the four measurements in the morning and afternoon sessions. The averaged arterial T_1 values were 1908+/−77 ms for female participants (n = 6, Hct = 0.39+/−0.03, ctHb = 13.2±1.0 g/dL), and 1785+/−55 ms for male participants (n = 7, Hct = 0.45+/−0.02, ctHb = 15.1±1.0 g/dL). For all the participants combined (n = 13, Hct = 0.42+/−0.04, ctHb = 14.2±1.4 g/dL), the averaged arterial T_1 value of 1841+/−89 ms was 56+/−35 ms longer than the average venous T_1 value of 1785+/−80 ms. The in vitro arterial T_1 values from 9 subjects are also listed in Table 1.

As shown in the scatter plot (Fig. 3a) and Bland-Altman (Fig. 3b) plots, reasonable correlation and agreement between arterial T_1 values measured *in vivo* and *in vitro* were found with a correlation coefficient of 0.78. Additionally, the *in vivo* arterial T_1 values were found to differ significantly ($P = 6.1\times10^{-5}$) from the *in vivo* venous T_1 values (Fig. 3c). As expected, the arterial T_1 values measured *in vivo* correlated significantly with Hct (Fig. 4a and Eq. [6]) as well as with ctHb (Fig. 4b and Eq. [7]).

$$1000/\mathrm{T_{1a}}\,(\mathrm{ms}) = 0.625 \times \mathrm{Hct} + 0.280 \quad [6]$$

$$1000/\mathrm{T_{1a}}\,(\mathrm{ms}) = 0.016 \times \mathrm{ctHb(g/dL)} + 0.317 \quad [7]$$

In the reproducibility study, the intra-session CoV was 1.1%, which reflects the low measurement noise and high reliability of this technique. The inter-session CoV was 2.1%, which is a little higher than intra-session CoV. We tentatively attribute this to possible physiological fluctuation (e.g. fluid intake) between morning and afternoon. The inter-subject CoV was 5.6%, which reflects the physiological differences (e.g. in Hct) between different subjects.

Discussion

A new approach for rapid measurement of T_1 values from the ICA at 3T was presented through optimization of body positioning, inversion pulse type and acquisition scheme of a previous protocol to measure blood T_1 in the IJV (12). Specifically, the subjects were centered at the clavicle, and an inversion pulse (HS4) with reduced sensitivity to B_0/B_1 inhomogeneity was employed to ensure effective inversion of the magnetization of feeding arterial blood. Furthermore, TFE acquisition with large flip angles was used to suppress the background signal while maintaining high SNR. The accuracy of our *in vivo* method was validated by comparing the measured T_1 values with *in vitro* data. Low intra-session and inter-session CoVs, 1.1% and 2.1% respectively, indicated excellent precision and reproducibility.

The measured arterial blood T_1 values of males (1785+/−55 ms, Hct = 0.45+/−0.02) agree well with a previous arterial T_1 study on the abdominal aorta of male subjects (1779+/−80 ms with Hct = 0.47+/−0.03) using a traditional inversion-recovery method (11). For both females and males, the measured arterial blood T_1 values (1841+/−89 ms, Hct = 0.42+/−0.04, Table 1) are close to the arterial value predicted from our recent theoretical T_1 model (1839 ms, Supporting Table S1) (19) and another model calibrated from *in vivo* data (1771 ms) (38) for normal blood (Hct = 0.42, Y = 100%, and f_{MetHb} = 1.0%,), but are about 200 ms longer than the widely adopted value (1664 ms with Hct = 0.42) based on bovine blood experiments (13). This ~200 ms difference is partly due to a higher level of MetHb in bovine samples. The bovine blood had about ~2% MetHb vs. 1.0+/−0.2% for the human blood sampled in this study (Table 1). According to the T_1 model (19), an increase of 1% in MetHb induces ~100 ms shortening in blood T_1 (Supporting Table S1).

The blood T_1 values measured at the ICA were 56+/−35 ms longer than the ones at the IJV (Table 1, Fig. 3c). Interestingly, when using the T_1 model (19), the T_1 values of arterial (Y: 100%) and venous (Y: 65%) blood were predicted as 1839 ms and 1681 ms, respectively, with a 158 ms difference between them (Supporting Table S1). One possible explanation for the smaller difference of arterial-venous T_1 values observed in this study may be related to the fact that some portion of the blood contributing to the later part of the inversion recovery curve originated from the capillary compartment. Note that the microvascular Hct in capillaries is known to be approximately 75%–85% of that for large vessels (Fahraeus effect) (39,40). Based on our T_1 model (19), a lower Hct level (e.g., Hct = 0.80 × 0.42 = 0.34) with increased oxygenation fraction (e.g., Y = (100% + 65%)/2 = 82%) gives an increased blood T_1, yielding a capillary T_1 of 1857 ms (Supporting Table S1), which is close to our theoretical arterial T_1 (1839 ms, Supporting Table S1). Accordingly, this contamination of blood from capillaries may augment the T_1 estimated at IJV but negligibly impact the T_1 measurement at ICA. Although shortening the repetition time of the employed inversion recovery sequence would be desirable to reduce this bias, the data acquired at longer TIs are close to the equilibrium magnetization and could allow T_1 fitting more robust against physiology noise.

Other possible causes of the lower arterial T_1 may be incomplete refreshing of spins or inhomogeneous inversion for the chest. We think we can exclude the first based on

arguments in the methods section for spin history, but incomplete inversion coverage of the thoracic cavity where the blood supply for the ICA is located may be possible. However, the arterial T_1 values agree well with *in vitro* data (Fig. 3a,b, Table 1), which suggests that this was not a significant source of error in this study. Admittedly, for regular neuroimaging studies, the described method for obtaining arterial T_1 values by repositioning to the subject's clavicle is not as efficient and convenient as the protocols for measuring venous T_1 (8,12,15). Therefore, when scanning a person with normal blood composition, one alternative could be to first measure the T_1 at IJV (12), and then empirically add 56 ms found in this study to estimate the arterial T_1 value.

The significant difference of arterial blood T_1 values found between female and male adults (1908±77 ms vs. 1785+/−55 ms) was shown to be associated with the gender difference of their Hct values (0.39+/−0.03 vs. 0.45+/−0.02) (Table 1, Fig. 4a). As demonstrated in previous studies (7–19) on both arterial and venous blood, the blood relaxation rate $1/T_1$ has a linear dependence on Hct. Earlier work (10,19,20) has asserted hemoglobin as the main source of the T_1 relaxation in arterial blood. Indeed, the good correlation of $1/T_1$ and Hct is due to the narrow distribution of the mean corpuscular hemoglobin concentration (MCHC), which is the concentration of hemoglobin in erythrocytes and ranges from 32~36 g/dL in normal blood (41). Therefore, the correlation (Fig 4b) between the $1/T_1$ and ctHb (ctHb = Hct · MCHC) is more instructive, especially for the abnormal blood such as sickle cell disease where erythrocytes are severely dehydrated and MCHC is elevated (42).

One question is whether pulsatile flow may still significantly affect the measured T_1. We do not think so because during the interval (T_d in Figure 1) between adjacent TFE acquisitions, all blood in the imaging plane will be refreshed even at the diastolic rate. Future cardiac-gated measurements could provide more insight into this. However, pulsatile flow may affect image quality because we only had first order flow compensation during the acquisition. Indeed, we saw improvements in the images when replacing the segmented EPI acquisitions used in our previous IJV T_1 paper to the current segmented TFE acquisitions.

Knowledge of the arterial T_1 is critical for quantitative CBF mapping with ASL (6,43,44) and CBV studies with VASO (4,5,45). It is known that CBF values estimated using ASL are negatively correlated with the arterial blood T_1 values (6). Currently, the arterial blood T_1 of the healthy adults to be used for the quantification of ASL data is recommended as 1650 ms (13) at 3.0T. For the highest arterial blood T_1 value obtained in this study (2037 ms, Hct: 0.36), using this 18% undervalued blood T_1 (1650 ms) would cause a 35% overestimation of CBF. Similarly, the inversion time in VASO experiment will be underestimated by 18% and thus cause a 70% overestimation of ΔCBV.

Conclusion

We demonstrated a fast technique (~1 min) for accurately and reliably measuring arterial blood T_1 at the ICA. The proposed method can be performed individually to avoid possible inaccuracies due to Hct variation or abnormal blood composition. When not performing such a measurement, we recommend the use of 1908 ms and 1785 ms for healthy female and male adults or 1841 ms for adults in general, or estimating the arterial blood T_1 values based

on Eqs. [6] or [7] if Hct or ctHb are known for subjects with normal blood composition. The combination of our method with ASL and VASO techniques can result in more accurate estimation of CBF and CBV, especially for the patients with blood disorders.

Supplementary Material

Refer to Web version on PubMed Central for supplementary material.

Acknowledgments

Grant support: NIH: P41 EB015909; NIH: K25 HL121192; NIH: R01 MH084021

References

1. Detre JA, Leigh JS, Williams DS, Koretsky AP. Perfusion imaging. Magn Reson Med. 1992; 23:37–45. [PubMed: 1734182]
2. Lu H, Golay X, Pekar JJ, Van Zijl PCM. Functional magnetic resonance imaging based on changes in vascular space occupancy. Magn Reson Med. 2003; 50:263–274. [PubMed: 12876702]
3. Hua J, Qin Q, Donahue MJ, Zhou J, Pekar JJ, van Zijl PCM. Inflow-based vascular-space-occupancy (iVASO) MRI. Magn Reson Med. 2011; 66:40–56. [PubMed: 21695719]
4. Donahue MJ, Sideso E, MacIntosh BJ, Kennedy J, Handa A, Jezzard P. Absolute arterial cerebral blood volume quantification using inflow vascular-space-occupancy with dynamic subtraction magnetic resonance imaging. J Cereb blood flow Metab. 2010; 30:1329–42. [PubMed: 20145656]
5. Hua J, Qin Q, Pekar JJ, van Zijl PCM. Measurement of absolute arterial cerebral blood volume in human brain without using a contrast agent. NMR Biomed. 2011; 24:1313–25. [PubMed: 21608057]
6. Alsop DC, Detre JA, Golay X, et al. Recommended implementation of arterial spin-labeled perfusion MRI for clinical applications: A consensus of the ISMRM perfusion study group and the European consortium for ASL in dementia. Magn Reson Med. 2015; 73:102–116. [PubMed: 24715426]
7. De Vis JB, Hendrikse J, Groenendaal F, de Vries LS, Kersbergen KJ, Benders MJNL, Petersen ET. Impact of neonate haematocrit variability on the longitudinal relaxation time of blood: Implications for arterial spin labelling MRI. NeuroImage Clin. 2014; 4:517–525. [PubMed: 24818078]
8. Varela M, Hajnal JV, Petersen ET, Golay X, Merchant N, Larkman DJ. A method for rapid in vivo measurement of blood T1. NMR Biomed. 2011; 24:80–8. [PubMed: 20669148]
9. Grgac K, van Zijl PCM, Qin Q. Hematocrit and oxygenation dependence of blood (1)H2O T1 at 7 tesla. Magn Reson Med. 2013; 70:1153–1159. [PubMed: 23169066]
10. Blockley NP, Jiang L, Gardener AG, Ludman CN, Francis ST, Gowland PA. Field strength dependence of R1 and R2* relaxivities of human whole blood to ProHance, Vasovist, and deoxyhemoglobin. Magn Reson Med. 2008; 60:1313–1320. [PubMed: 19030165]
11. Shimada K, Nagasaka T, Shidahara M, Machida Y, Tamura H. In vivo measurement of longitudinal relaxation time of human blood by inversion-recovery fast gradient-echo MR imaging at 3T. Magn Reson Med Sci. 2012; 11:265–71. [PubMed: 23269013]
12. Qin Q, Strouse JJ, van Zijl PCM. Fast measurement of blood T1 in the human jugular vein at 3 Tesla. Magn Reson Med. 2011; 65:1297–304. [PubMed: 21500258]
13. Lu H, Clingman C, Golay X, van Zijl PCM. Determining the longitudinal relaxation time (T1) of blood at 3.0 Tesla. Magn Reson Med. 2004; 52:679–82. [PubMed: 15334591]
14. Silvennoinen MJ, Kettunen MI, Kauppinen RA. Effects of hematocrit and oxygen saturation level on blood spin-lattice relaxation. Magn Reson Med. 2003; 49:568–71. [PubMed: 12594761]
15. Wu WC, Jain V, Li C, Giannetta M, Hurt H, Wehrli FW, Wang DJJ. In vivo venous blood T1 measurement using inversion recovery true-FISP in children and adults. Magn Reson Med. 2010; 64:1140–7. [PubMed: 20564586]

16. Liu P, Chalak LF, Krishnamurthy LC, Mir I, Peng S, Huang H, Lu H. T1 and T2 values of human neonatal blood at 3 Tesla: Dependence on hematocrit, oxygenation, and temperature. Magn Reson Med. 2016; 75:1730. [PubMed: 25981985]
17. Rane SD, Gore JC. Measurement of T1 of human arterial and venous blood at 7T. Magn Reson Imaging. 2013; 31:477–9. [PubMed: 23102945]
18. Bryant RG, Marill K, Blackmore C, Francis C. Magnetic relaxation in blood and blood clots. Magn Reson Med. 1990; 13:133–144. [PubMed: 2319929]
19. Li W, Grgac K, Huang A, Yadav N, Qin Q, van Zijl PCM. Quantitative theory for the longitudinal relaxation time of blood water. Magn Reson Med. 2015 Epub ahead of print.
20. Brooks RA. Magnetic resonance imaging of stationary blood: A review. Med Phys. 1987; 14:903. [PubMed: 3696078]
21. Thulborn KR, Waterton JC, Matthews PM, Radda GK. Oxygenation Dependence of the Transverse Relaxation Time of Water Protons in Whole Blood at High Field. Biochim Biophys Acta. 1982; 714:265–270. [PubMed: 6275909]
22. Atalay MK, Reeder SB, Zerhouni EA, Forder JR. Blood oxygenation dependence of T1 and T2 in the isolated, perfused rabbit heart at 4.7T. Magn Reson Med. 1995; 34:623–627. [PubMed: 8524032]
23. Silvennoinen MJ, Clingman CS, Golay X, Kauppinen RA, van Zijl PCM. Comparison of the dependence of blood R2 and R2* on oxygen saturation at 1.5 and 4.7 Tesla. Magn Reson Med. 2003; 49:47–60. [PubMed: 12509819]
24. Gomori J, Grossman R, Yuip C, Asakura T. NMR relaxation times of blood: dependence on field strength, oxidation state, and cell integrity. J Comput Assist Tomogr. 1987; 11:684–690. [PubMed: 3597895]
25. Lin AL, Qin Q, Zhao X, Duong TQ. Blood longitudinal (T1) and transverse (T2) relaxation time constants at 11.7 Tesla. Magn Reson Mater Phys Biol Med. 2012; 25:245–249.
26. Lindstrom TR, Koenig SH. Magnetic-field-dependent water proton spin-lattice relaxation rates of hemoglobin solutions and whole blood. J Magn Reson. 1974; 15:344–353.
27. Niendorf E, Grist T, Lee F, Brazy P, Santyr G. Rapid in vivo measurement of single kidney extraction fraction and glomerular filtration rate with MR imaging. Radiology. 1998; 206:791–798. [PubMed: 9494503]
28. Dumoulin CL, Buonocore MH, Opsahl LR, Katzberg RW, Darrow RD, Morris TW, Batey C. Noninvasive measurement of renal hemodynamic functions using gadolinium enhanced magnetic resonance imaging. Magn Reson Med. 1994; 32:370–8. [PubMed: 7984069]
29. Zhang X, Petersen ET, Ghariq E, De Vis JB, Webb AG, Teeuwisse WM, Hendrikse J, van Osch MJP. In vivo blood T1 measurements at 1.5 T, 3 T, and 7 T. Magn Reson Med. 2013; 70:1082–1086. [PubMed: 23172845]
30. Schreiber SJ, Kauert A, Doepp F, Valdueza JM. Measurement of global cerebral circulation time using power duplex echo-contrast bolus tracking. Cerebrovasc Dis. 2003; 15:129–32. [PubMed: 12499722]
31. Jones RH, Sabiston DC, Bates BB, Morris JJ, Anderson PA, Goodrich JK. Quantitative radionuclide angiocardiography for determination of chamber to chamber cardiac transit times. Am J Cardiol. 1972; 30:855–64. [PubMed: 4634283]
32. Francois CJ, Shors SM, Bonow RO, Finn JP. Analysis of cardiopulmonary transit times at contrast material-enhanced MR imaging in patients with heart disease. Radiology. 2003; 227:447–52. [PubMed: 12676971]
33. Silver M, Joseph R, Hoult D. Highly selective and π pulse generation. J Magn Reson. 1984; 59:347–351.
34. Tannús, a, Garwood, M. Improved performance of frequency-swept pulses using offset-independent adiabaticity. J Magn Reson. 1996; 120:133–137.
35. Hwang TL, van Zijl PC, Garwood M. Fast broadband inversion by adiabatic pulses. J Magn Reson. 1998; 133:200–3. [PubMed: 9654487]
36. Liu P, Xu F, Lu H. Test-retest reproducibility of a rapid method to measure brain oxygen metabolism. Magn Reson Med. 2013; 69:675–81. [PubMed: 22517498]

37. Sung K, Nayak KS. Design and use of tailored hard-pulse trains for uniformed saturation of myocardium at 3 Tesla. Magn Reson Med. 2008; 60:997–1002. [PubMed: 18816833]

38. Hales PW, Kirkham FJ, Clark CA. A general model to calculate the spin-lattice (T1) relaxation time of blood, accounting for haematocrit, oxygen saturation and magnetic field strength. J Cereb Blood Flow Metab. 2016; 36:370–374. [PubMed: 26661147]

39. Phelps M, Huang S, Hoffman E, Kuhl D. Validation of tomorgraphic measurement of cerebral blood-volume with C-11 labeled carboxyhemoglobin. J Nucl Med. 1979; 20:328–334. [PubMed: 119833]

40. Sakai F, Nakazawa K, Tazaki Y, Ishii K, Hino H, Igarashi H, Kanda T. Regional cerebral blood volume and hematocrit measured in normal human volunteers by single-photon emission computed tomography. J Cereb Blood Flow Metab. 1985; 5:207–13. [PubMed: 3921557]

41. Chanarin, I., Brozovic, M., Tidmarsh, E., Waters, D. Blood and its disease. New York: Churchill Livingstone; 1984.

42. Clark MR. Mean corpuscular hemoglobin concentration and cell deformability. Ann N Y Acad Sci. 1989; 565:284–94. [PubMed: 2672965]

43. Jain V, Duda J, Avants B, Giannetta M, Xie SX, Roberts T, Detre JA, Hurt H, Wehrli FW, Wang DJJ. Longitudinal reproducibility and accuracy of pseudo-continuous arterial spin-labeled perfusion MR imaging in typically developing children. Radiology. 2012; 263:527–36. [PubMed: 22517961]

44. Wu W-C, St Lawrence KS, Licht DJ, Wang DJJ. Quantification issues in arterial spin labeling perfusion magnetic resonance imaging. Top Magn Reson Imaging. 2010; 21:65–73. [PubMed: 21613872]

45. Lu H, Hua J, van Zijl PCM. Noninvasive functional imaging of cerebral blood volume with vascular-space-occupancy (VASO) MRI. NMR Biomed. 2013; 26:932–48. [PubMed: 23355392]

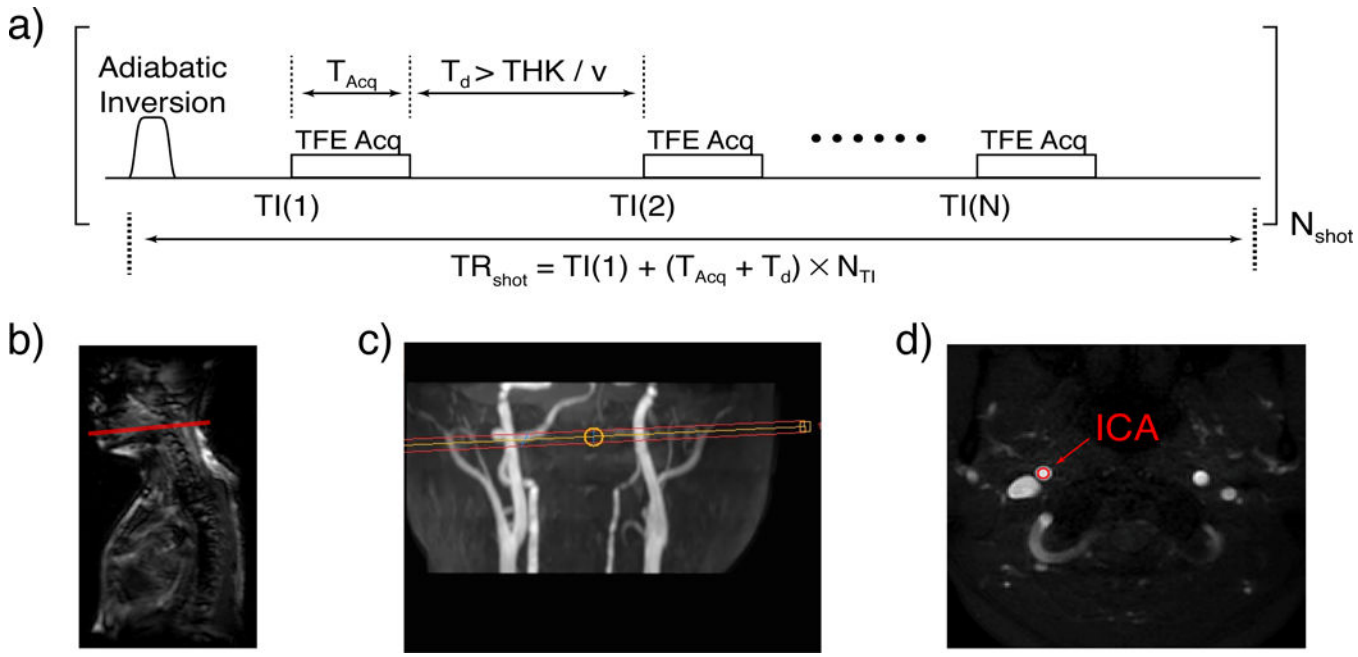

Figure 1.

a) Pulse diagram for measuring arterial T_1. Following an adiabatic 180° inversion pulse, a series TFE acquisitions are used to sample the inversion recovery curve with an interval that allows the blood magnetization to refresh in the imaging plane. THK=slice thickness; v=blood velocity. b) The survey image shows the B_1 coverage of the whole upper torso when centered at clavicle. c) Time of flight angiographic scout image. The red box indicates the imaging slice chosen to the ICA. d) one representative image from the fast T_1 protocol (TI=9850ms).

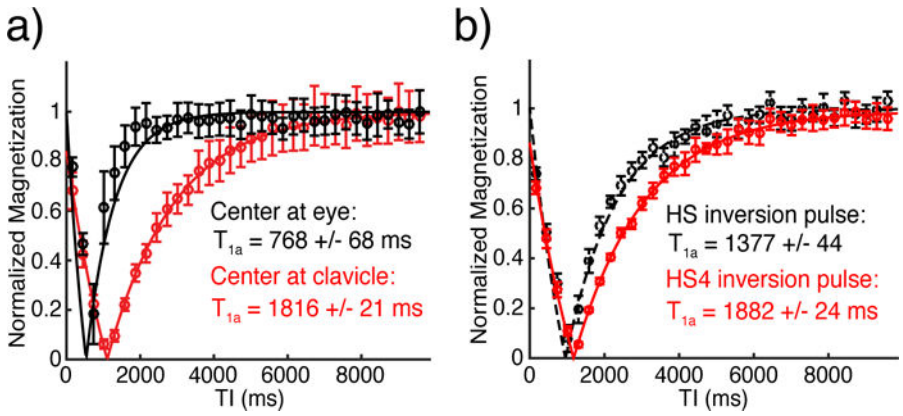

Figure 2.

a) Inversion recovery curves measured at the same subject with the same pulse sequence but with the subject positioned at the eye (black line) and at the clavicle (red line). b) Inversion recovery curves measured using HS and HS4 inversion pulses with the same subject positioned at the clavicle.

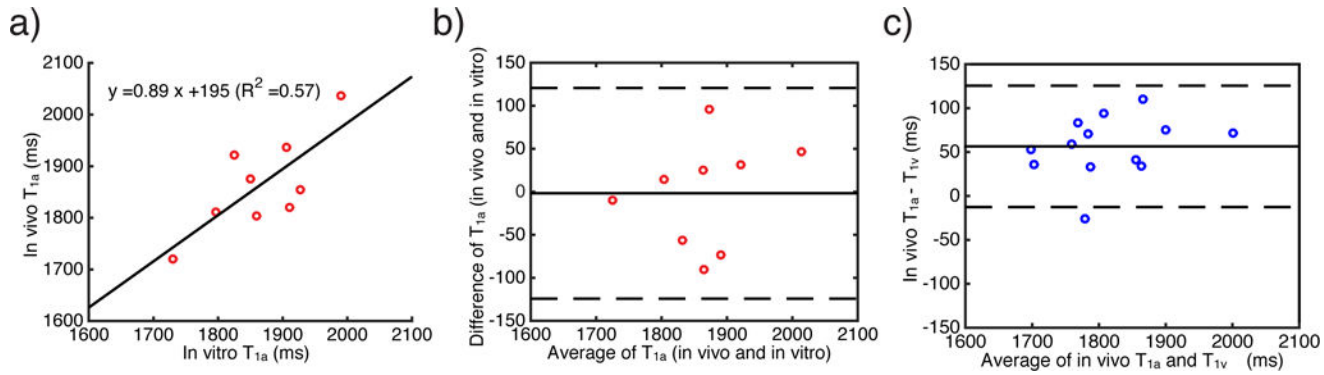

Figure 3.

a) correlation and b) agreement (Bland-Altman plot) between arterial blood T_1 values measured in vivo and in vitro. In a), the solid line is a linear fit of the arterial blood T_1 values measured in vivo vs in vitro. In b), the solid line indicates the mean difference between arterial blood T_1 values measured in vivo vs in vitro at the same subject, and the dashed lines represent two times the standard deviation from the mean difference. c) Bland-Altman plot to compare arterial and venous T_1 measured in vivo. The solid line indicates the mean difference between arterial blood T_1 and venous blood T_1, and the dashed lines represent two times the standard deviation from the mean difference.

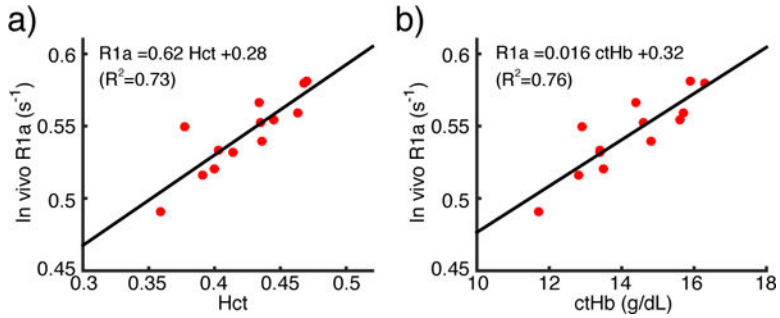

Figure 4.

Linear relationship between the arterial longitudinal relaxation rate ($R_{1a} = 1/T_{1a}$) and Hct (a) and ctHb (b).

Table 1

The arterial T_1 measured from internal carotid artery and in vitro for different subjects.

Subject		Hct	ctHb (g/dL)	$T_{1a,in\ vivo}$ (ms)	$T_{1v,in\ vivo}$ (ms)	f_{MetHb}	$T_{1a,in\ vitro}$ (ms)
1	Female	0.40	13.4	1876±19	1835±32	1.0%	1851±19
2	Female	0.40	13.5	1921±41	1811±37	0.9%	1825±41
3	Female	0.36	11.7	2037±26	1966±28	1.0%	1990±26
4	Female	0.44	14.8	1854±28	1760±35	0.9%	1927±28
5	Female	0.38	12.9	1820±30	1749±27	1.0%	1910±30
6	Female	0.39	12.8	1937±53	1862±70	1.1%	1906±53
7	Male	0.47	15.9	1720±26	1685±34	0.6%	1730±26
8	Male	0.45	15.6	1804±61	1771±17	1.1%	1806±61
9	Male	0.44	14.6	1811±30	1727±37	1.0%	1797±30
10	Male	0.47	16.3	1725±41	1672±15		
11	Male	0.41	13.4	1880±17	1846±18		
12	Male	0.46	15.7	1789±24	1730±8		
13	Male	0.43	14.4	1766±21	1792±13		
Female Mean±SD		0.39±0.03	13.2±1.0	1908±77	1831±79	1.0±0.1%	1902±58
Male Mean±SD		0.45±0.02	15.1±1.0	1785±55	1746±61	0.9±0.3%	1778±41
Total Mean±SD		0.42±0.04	14.2±1.4	1841±89	1785±80	1.0±0.2%	1860±80